J|A|C|S
ARTICLES
Published on Web 02/11/2006

BF_3-Activated Oxidation of Alkanes by MnO_4^-

William W. Y. Lam,[†] Shek-Man Yiu,[†] Joyce M. N. Lee,[†] Sammi K. Y. Yau,[†] Hoi-Ki Kwong,[†] Tai-Chu Lau,*[,†] Dan Liu,[‡] and Zhenyang Lin*[,‡]

Contribution from the Department of Biology and Chemistry, City University of Hong Kong, Tat Chee Avenue, Kowloon Tong, Hong Kong, China, and Department of Chemistry, The Hong Kong University of Science and Technology, Clear Water Bay, Kowloon, Hong Kong, China

Received August 13, 2005; E-mail: bhtclau@cityu.edu.hk; chzlin@ust.hk

Abstract: The oxidation of alkanes and arylalkanes by $KMnO_4$ in CH_3CN is greatly accelerated by the presence of just a few equivalents of BF_3, the reaction occurring readily at room temperature. Carbonyl compounds are the predominant products in the oxidation of secondary C−H bonds. Spectrophotometric and kinetics studies show that BF_3 forms an adduct with $KMnO_4$ in CH_3CN, $[BF_3{\cdot}MnO_4]^-$, which is the active species responsible for the oxidation of C−H bonds. The rate constant for the oxidation of toluene by $[BF_3{\cdot}MnO_4]^-$ is over 7 orders of magnitude faster than by MnO_4^- alone. The kinetic isotope effects for the oxidation of cyclohexane, toluene, and ethylbenzene at 25.0 °C are as follows: $k_{C_6H_{12}}/k_{C_6D_{12}} = 5.3 \pm 0.6$, $k_{C_7H_8}/k_{C_7D_8} = 6.8 \pm 0.5$, $k_{C_8H_{10}}/k_{C_8D_{10}} = 7.1 \pm 0.5$. The rate-limiting step for all of these reactions is most likely hydrogen-atom transfer from the substrate to an oxo group of the adduct. A good linear correlation between log(rate constant) and C−H bond energies of the hydrocarbons is found. The accelerating effect of BF_3 on the oxidation of methane by MnO_4^- has been studied computationally by the Density Functional Theory (DFT) method. A significant decrease in the reaction barrier results from BF_3 coordination to MnO_4^-. The BF_3 coordination increases the ability of the Mn metal center to achieve a d^1 Mn(VI) electron configuration in the transition state. Calculations also indicate that the species $[2BF_3{\cdot}MnO_4]^-$ is more reactive than $[BF_3{\cdot}MnO_4]^-$.

Introduction

Enzymes such as cytochrome P-450 and methane monooxygenases are able to oxidize unactivated C−H bonds under mild conditions.[1−3] The search for highly reactive metal-oxo species in chemical systems that can mimic the reactivity of the iron-oxo intermediates in these enzymes remains a challenge to chemists.[4−8] Metal-oxo species such as chromate and permanganate have long been used as oxidants for a variety of organic functional groups.[9] However, their use in the oxidation of alkanes is limited; refluxing conditions are often required to oxidize unactivated C−H bonds. Our approach to generate highly oxidizing reagents is to make use of Lewis acids to activate metal-oxo species. The activating effects of Brønsted acids on metal-oxo species are well-known; however the use of Lewis acids to enhance the reactivity of these species is much less studied. We have recently reported that the oxidation of alkanes by anionic oxo species of ruthenium,[10] iron,[11] manganese,[12] chromium,[12] and osmium[13] is greatly enhanced by Lewis acids. The Lewis acid assisted oxidation of various other organic substrates by permanganate has also been subsequently reported by Lee and co-workers.[14,15] Mayer and co-workers have recently studied the kinetics and mechanisms of the oxidation of various arylalkanes by $^n Bu_4NMnO_4$ in organic solvents.[16−18] We report here a kinetics and mechanistic study of the BF_3-activated oxidation of alkanes and arylalkanes by $KMnO_4$. Our results show that BF_3 forms an adduct with MnO_4^- in CH_3CN that oxidizes hydrocarbons at rates over 7 orders of magnitude faster than that by MnO_4^- alone. Initial results of this work have been communicated.[12] The accelerating effect of BF_3 on the oxidation of methane by MnO_4^- has been studied computationally by the Density Functional Theory (DFT) method.

[†] City University of Hong Kong.
[‡] The Hong Kong University of Science and Technology.

(1) Ortiz de Montellano, P. R., Ed. *Cytochrome P450. Structure, Mechanism and Biochemistry*; Plenum Press: New York, 1995.
(2) McLain, J. L.; Lee, J.; Groves, J. T. In *Biomimetic Oxidations Catalyzed by Transition Metal Complexes*; Meunier, B., Ed.; Imperial College Press: London, 2000; pp 91−170.
(3) Baik, M.-H.; Newcomb, M.; Friesner, R. A.; Lippard, S. J. *Chem. Rev.* **2003**, *103*, 2385−2420.
(4) Hu, Z.; Gorun, S. M. In *Biomimetic Oxidations Catalyzed by Transition Metal Complexes*; Meunier, B., Ed.; Imperial College Press: London, 2000; pp 269−308.
(5) Robert, A.; Meunier, B. In *Biomimetic Oxidations Catalyzed by Transition Metal Complexes*; Meunier, B., Ed.; Imperial College Press: London, 2000; pp 543−562.
(6) Shilov, A. E.; Shul'pin, G. B. *Chem. Rev.* **1997**, *97*, 2879−2932.
(7) Crabtree, R. H. *J. Chem. Soc., Dalton Trans.* **2001**, 2437−2450.
(8) Fokin, A. A.; Schreiner, P. R. *Chem. Rev.* **2002**, *102*, 1551−1594.
(9) Hudlicky, M. *Oxidations in Organic Chemistry*; American Chemical Society: Washington, DC, 1990.
(10) Lau, T. C.; Mak, C. K. *J. Chem. Soc., Chem. Commun.* **1993**, 766−767.
(11) Ho, C. M.; Lau, T. C. *New J. Chem.* **2000**, *24*, 587−590.
(12) Lau, T. C.; Wu, Z. B.; Bai, Z. L.; Mak, C. K. *J. Chem. Soc., Dalton Trans.* **1995**, 695−696.
(13) Yiu, S. M.; Wu, Z. B.; Mak, C. K.; Lau, T. C. *J. Am. Chem. Soc.* **2004**, *126*, 14921−14929.
(14) Xie, N.; Binstead, R. A.; Block, E.; Chandler, W. D.; Lee, D. G.; Meyer, T. J.; Thiruvazhi, M. *J. Org. Chem.* **2000**, *65*, 1008−1015.
(15) Lai, S.; Lee, D. G. *Tetrahedron* **2002**, *58*, 9879−9887.
(16) Gardner, K. A.; Mayer, J. M. *Science* **1995**, *269*, 1849−1851.
(17) Gardner, K. A.; Kuehnert, L. L.; Mayer, J. M. *Inorg. Chem.* **1997**, *36*, 2069−2078.
(18) Mayer, J. M. *Acc. Chem. Res.* **1998**, *31*, 441−450.

Experimental Section

Materials. CAUTION: *Care should be taken in handling BF_3/MnO_4^- in organic solvents, since the system is very reactive. Although we have not encountered any problems so far, the amount of $KMnO_4$/$^nBu_4NMnO_4$ used each time should be less than 50 mg.* Potassium permanganate (Ajax Chemicals, AR) was used as received. $^nBu_4NMnO_4$ was prepared according to a literature method.[14] A Boron trifluoride−acetonitrile complex solution (BF_3·CH_3CN) (Fluka, 15−18%) was stored at −20 °C and was used without further purification. The concentration was determined to be 15.2% by hydrolysis to H_3BO_3 and HF followed by titration with NaOH. *p*-Xylene (Aldrich, 99+% anhydrous), 4-methylanisole (Aldrich, 99%), 4-chlorotoluene (Aldrich, 98% GC), d_8-toluene (Aldrich, 99.5 at. %D), d_{10}-ethylbenzene (Acrôs, 98+ at. %D), and d_{12}-cyclohexane (Aldrich, 99.5 at. %D) were used as received. Cyclohexane (Lab-scan, AR), cycloheptane (Aldrich, 98%), cyclooctane (Aldrich, 99%), cyclopentane (Lab-scan, AR), toluene (Riedel-deHaën, 99.7%), ethylbenzene (Riedel-deHaën, 99%), and cumene (Merck) were washed with cold concentrated H_2SO_4 followed by distilled water and then 5% aqueous $NaHCO_3$. They were then dried with $MgSO_4$ and distilled from CaH_2 under argon. They were passed through a column of alumina before use. Triphenylmethane (Aldrich, 99%) was recrystallized from ethanol. Diphenylmethane (Aldrich, 99%) was sublimed before use. Acetonitrile (Lab-scan, AR) was stirred overnight with $KMnO_4$ and then distilled; it was distilled again over CaH_2 under argon.[19]

Oxidation of Hydrocarbons. A solution of BF_3·CH_3CN in CH_3CN was added with vigorous stirring to a solution of $KMnO_4$ (0.02 mmol) in CH_3CN containing cyclohexane. After 5 min 100 μL of H_2O were added, and the resulting mixture was analyzed by GC and GC−MS using chlorobenzene as the internal standard. A Hewlett-Packard 6890 gas chromatograph with an FFAP capillary column was used. GC−MS measurements were carried out on an HP 6890 gas chromatograph interfaced to an HP 5973 mass selective detector.

Manganese Oxidation State Determination. The oxidation state of the manganese product was determined by an iodometric method.[20] The manganese oxidation state was found to be 3.94 ± 0.16 in the oxidation of cyclohexane.

Kinetics. The kinetics of the reaction were studied by using a Hewlett-Packard 8452A UV−vis spectrophotometer or an Applied Photophysics DX-17MV stopped-flow spectrophotometer. The concentrations of the hydrocarbons were at least in 10-fold excess of that of MnO_4^-. Reactions were initiated by mixing BF_3·CH_3CN in CH_3CN with a freshly prepared solution of $KMnO_4$ and hydrocarbon in CH_3CN under argon. The reaction progress was monitored by observing absorbance changes at 526 nm (λ_{max} of MnO_4^-). Pseudo-first-order rate constants, k_{obs}, were obtained by nonlinear least-squares fits of A_t vs time t according to the equation $A_t = A_f + (A_0 - A_f)\exp(-k_{obs}t)$, where A_0 and A_f are the initial and final absorbances, respectively.

Kinetic Isotope Effects (KIEs). The KIEs for cyclohexane oxidation were studied by using an equimolar mixture of cyclohexane and d_{12}-cyclohexane as substrate. The products were analyzed by GC and GC−MS. The peaks due to the possible products cyclohexanol, d_{12}-cyclohexanol, cyclohexanone, and d_{10}-cyclohexanone are well resolved in the GC spectrum under our experimental conditions. The KIE was calculated by the following equation: $k_{C_6H_{12}}/k_{C_6D_{12}}$ = (moles of *c*-C_6H_{11}-OH + moles of *c*-$C_6H_{10}O$)/(moles of *c*-$C_6D_{11}OD$ + moles of *c*-$C_6D_{10}O$).

KIEs for cyclohexane, toluene, and ethylbenzene were also determined by comparing the rate constants for the oxidation of the protio vs deutero substrates using UV/vis spectrophotometric methods.

Results and Discussion

Oxidation of Cyclohexane by BF_3/MnO_4^-. In a typical experiment, a solution of BF_3·CH_3CN (8.6×10^{-2} M) in CH_3CN was added with vigorous stirring to a solution of $KMnO_4$ (4.3×10^{-3} M) containing cyclohexane (1.0 M) in CH_3CN at 23 °C. The purple color of solution was discharged within seconds. The oxidation state of the manganese after the reaction was determined to be 3.94 ± 0.16; this together with the appearance of a characteristic broad absorbance in the visible spectrum (vide infra) is consistent with the formation of colloidal MnO_2. Analysis of the organic products by GC and GC−MS after ca. 5 min indicated the presence of 8% cyclohexanol and 73% cyclohexanone.[21] The yields were calculated based on the system acting as a three-electron oxidant. No increase in yields were found by reducing the MnO_2 to Mn^{2+} using acidic iodide; apparently strong adsorption of products onto MnO_2 did not occur. In the absence of BF_3, $KMnO_4$ is stable in cyclohexane/CH_3CN for at least several hours at room temperature. The yields increased with the $[BF_3]/[MnO_4^-]$ ratio, the maximum yield occurring when 20 equiv of BF_3 were used (Figure 1, Table S1). The yields also increased significantly when the reaction was carried out in air instead of under argon (Figure 1, Table S2), indicating the intermediacy of cyclohexyl radicals. A few experiments were done using $^nBu_4NMnO_4$, and the yields were found to be similar to those using $KMnO_4$.

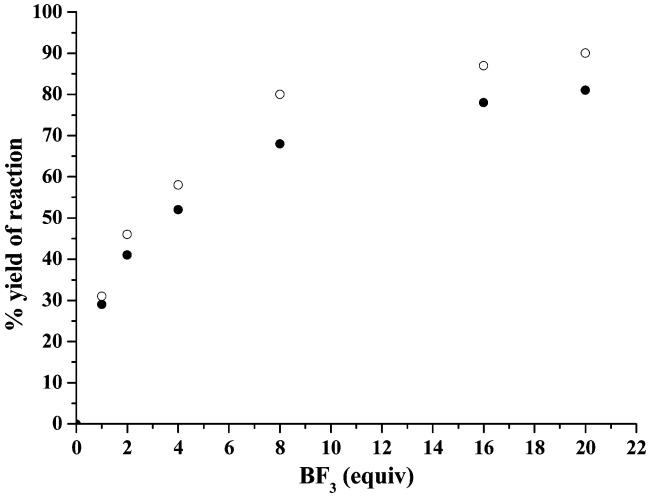

Figure 1. Plot of % yield vs $[BF_3]/[MnO_4^-]$ in the oxidation of cyclohexane by BF_3/MnO_4^-. (○) Reaction carried out in air. (●) Reaction carried out under argon. $[MnO_4^-] = 4.3 \times 10^{-3}$ M, [cyclohexane] = 1.0 M. The yields are calculated by assuming MnO_4^- acts as a three-electron oxidant: Yield = 100% × ($^2/_3$[cyclohexanol]$_f$ + $^4/_3$[cyclohexanone]$_f$)/$[MnO_4^-]_i$ (f = final, i = initial).

The kinetic isotope effects (KIE), determined from the competitive oxidation of cyclohexane and d_{12}-cyclohexane, were found to be 4.7 ± 0.5.

Spectrophotometric Changes. When BF_3·CH_3CN in CH_3CN (8.0×10^{-4} M) was mixed with $KMnO_4$ (1.0×10^{-4} M) in CH_3CN at 25.0 °C (in a two-compartment cuvette), there was an initial rapid decrease in absorbance in the region 500−580 nm, followed by a much slower and larger decay (Figure S1). The initial decay, which was too fast to be followed by stopped-flow spectrophotometry, corresponded to an apparent decomposition of ca. 15% MnO_4^-; however quenching of the reaction after about 5 s with excess acidic iodide followed by

(19) Armarego, W. L. F.; Perrin, D. D. *Purification of Laboratory Chemicals*, 4th ed.; Reed Educational and Professional Publishing Ltd.: Oxford, 1996.
(20) Lee, D. G.; Perez-Benito, J. F. *J. Org. Chem.* **1988**, *53*, 5725−5728.
(21) In the original communication BF_3·$MeCO_2H$ was used.[12] A lower yield of 42% cyclohexanone was obtained under different reaction conditions. We have also vigorously purified the solvent and substrates in the present study. BF_3·CH_3CN was used in the present study (instead of BF_3·$MeCO_2H$) to avoid complications from acetic acid.

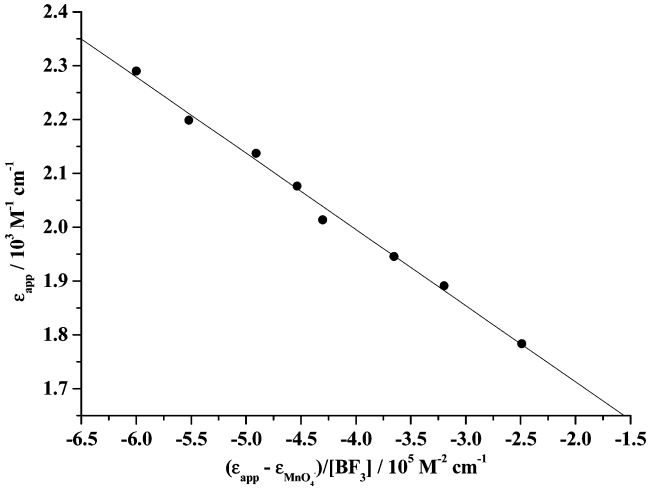

Figure 2. Plot of ϵ_{app} vs $(\epsilon_{app} - \epsilon_{MnO_4^-})/[BF_3]$ (slope $= -(1.42 \pm 0.06) \times 10^{-1}$, y-intercept $= (1.43 \pm 0.03)$, $r = -0.995$).

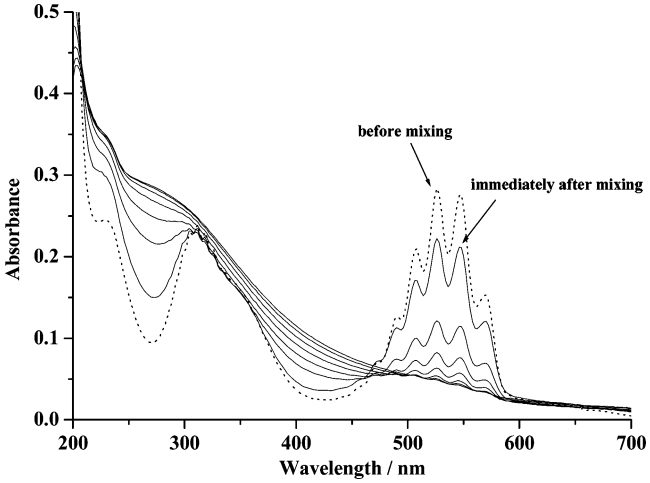

Figure 3. Spectrophotometric changes at 20-s intervals during the BF_3 (8×10^{-4} M) activated oxidation of cyclohexane (0.1 M) by MnO_4^- (1×10^{-4} M) in CH_3CN at 298.0 K.

measuring the concentration of I_3^- by UV−vis spectrophotometry indicated that over 95% of Mn^{VII} was still present. This decay also increased with the amount of BF_3. These results, together with other evidence presented below, suggest that the first rapid decay is due to the formation of a Lewis acid−base adduct as shown in eq 1, while the second step corresponds to decomposition of the adduct.

$$BF_3{\cdot}CH_3CN + MnO_4^- \overset{K}{\rightleftharpoons} [BF_3{\cdot}MnO_4]^- + CH_3CN \quad (1)$$

The equilibrium constant, K, for the adduct formation between MnO_4^- and BF_3 was determined by using a spectrophotometric method. A series of solutions were prepared by mixing 4×10^{-4} M $KMnO_4$ in CH_3CN with various amounts of $BF_3{\cdot}CH_3CN$ (4×10^{-4}−3×10^{-3} M), and the absorbance at 526 nm (A_{526}) of each solution in a 1-cm cell was taken immediately after mixing (within 5 s). The data were treated using eqs 2 and 3.[22]

$$\epsilon_{app} = \epsilon_{adduct} - \frac{\epsilon_{app} - \epsilon_{MnO_4^-}}{K[BF_3]} \quad (2)$$

$$\epsilon_{app} = A_{526}/[MnO_4^-]_i \quad (3)$$

ϵ_{app}, ϵ_{adduct}, $\epsilon_{MnO_4^-}$, and $[MnO_4^-]_i$ are the apparent molar absorptivity, molar absorptivity of the adduct, molar absorptivity of MnO_4^- (2530 M^{-1} cm^{-1} at 526 nm), and initial concentration of MnO_4^-, respectively. A plot of ϵ_{app} vs $(\epsilon_{app} - \epsilon_{MnO_4^-})/[BF_3]$ gives a straight line as shown in Figure 2, and from the slope K was determined to be 704 ± 31 M^{-1} at 25.0 °C. From the intercept ϵ_{adduct} (526 nm) was found to be 1430 ± 31 M^{-1} cm^{-1}. Attempts to detect the adduct $2BF_3{\cdot}MnO_4^-$ were problematic; at higher concentrations of BF_3 (>0.1 M) the decomposition of the adduct became very rapid.

Similar spectrophotometric changes occurred when BF_3 was added to $KMnO_4$ in the presence of cyclohexane, i.e., there was a very rapid decrease in absorbance, followed by a much slower decay (Figure 3). The change in absorbance for the first step increases with BF_3 concentration but is independent of cyclohexane concentration, consistent with the formation of the adduct $[BF_3{\cdot}MnO_4]^-$. The second step, however, is much faster than that in the absence of cyclohexane, and the rate also increases with cyclohexane concentration. The second step is assigned to the oxidation of cyclohexane by $[BF_3{\cdot}MnO_4]^-$. The optical spectra in the range 400−640 nm show the disappearance of MnO_4^- and the appearance of a broad absorbance due to colloidal MnO_2.[14,17]

Kinetics. The kinetics of the second step in the BF_3-activated oxidation of cyclohexane by MnO_4^- were monitored by observing the absorbance changes at 526 nm (λ_{max} of MnO_4^-). In the presence of at least 10-fold excess of BF_3 and cyclohexane, clean pseudo-first-order kinetics were observed for over three half-lives (Figure 4), despite the formation of MnO_2 colloids. First-order plots are usually slightly curved in oxidations by permanganate.[14,17] The pseudo-first-order rate constant, k_{obs}, is independent of the concentration of MnO_4^- (5×10^{-5}−2×10^{-4} M) but depends linearly on the concentration of the cyclohexane (1×10^{-3}−2×10^{-1} M) (Figure 4). The relatively small y-intercept of the second-order plot (1.02×10^{-3} s^{-1}) indicates that decomposition of $[BF_3{\cdot}MnO_4]^-$ is insignificant compared with the oxidation of cyclohexane. Attempts were also made to independently determine the rate constant for the decomposition of the adduct in the absence of cyclohexane. In this case the decay of the adduct appeared to be rather complicated and did not follow simple first-order kinetics, and a rate constant of approximately 2×10^{-3} s^{-1} (298.0 K, $[BF_3] = 2 \times 10^{-3}$ M) was obtained.

The effects of BF_3 on k_2 were studied by varying the concentration of BF_3 from 2×10^{-4} to 3×10^{-3} M, and saturation kinetics were observed (Figure 5). The kinetic results are consistent with an initial equilibrium formation of an adduct as shown in eq 1, followed by rate-limiting oxidation of cyclohexane by the adduct, as shown in eq 4.

$$[BF_3{\cdot}MnO_4]^- + c\text{-}C_6H_{12} \xrightarrow{k} \text{products} \quad (4)$$

k_2 is related to K and k by eq 5.

$$k_2 = \frac{kK[BF_3]}{1 + K[BF_3]} \quad (5)$$

(22) Ramette, R. W. *Chemical Equilibrium and Analysis*. Addison-Wesley Publishing Company, Ltd.: Massachusetts, 1981; pp 426−439.

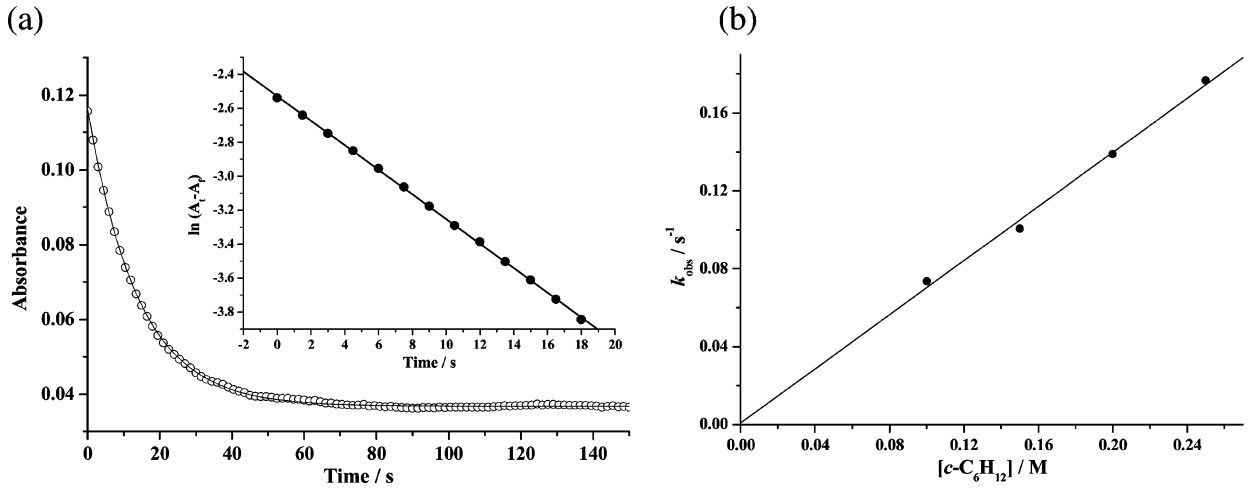

Figure 4. (a) Kinetic trace for the BF_3 (2×10^{-3} M) activated oxidation of cyclohexane (0.1 M) by MnO_4^- (5×10^{-5} M) in CH_3CN at 298.0 K. The inset shows the corresponding plot of $\ln(A_t - A_f)$ vs t (ca. three half-lives, slope = k_{obs}). (b) Second-order plot of k_{obs} vs [c-C_6H_{12}]. Slope = k_2 = (6.95 ± 0.38) × 10^{-1} M^{-1} s^{-1}, y-intercept = (1.03 ± 0.02) × 10^{-3} s^{-1}, r = 0.9971.

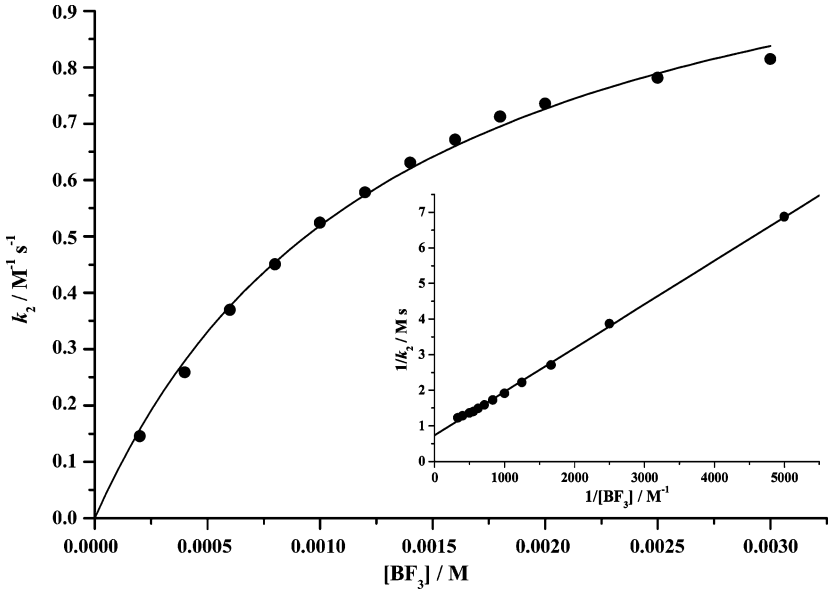

Figure 5. Plot of k_2 vs [BF_3] for the BF_3 activated oxidation of cyclohexane (0.10 M) by MnO_4^- (5×10^{-5} M) in CH_3CN at 298.0 K. The inset shows the corresponding plot of $1/k_2$ vs $1/[BF_3]$ (slope = (1.23 ± 0.01) × 10^{-3}, y-intercept = (7.33 ± 0.21) × 10^{-1}, r = 0.9996).

The plot of $1/k_2$ versus $1/K$ is linear (Figure 5); k and K are found to be (1.21 ± 0.03) M^{-1} s^{-1} and (752 ± 44) M^{-1} respectively at 25.0 °C by using a nonlinear least-squares fit of the data to eq 5. The value of K is in good agreement with the value 704 ± 31 M^{-1} obtained by direct spectrophotometric determination. The overall rate law is shown in eq 6.

$$v = \frac{kK[BF_3]}{1 + K[BF_3]}[MnO_4^-][c\text{-}C_6H_{12}] \qquad (6)$$

The maximum [BF_3] used in kinetic experiments was around 3×10^{-3} M. When higher concentrations were used the reactions became much faster and irreproducible. Experiments done at 0.1 M BF_3 indicated that k_2 is over 10 times larger than k, suggesting the existence of a more reactive species, which is probably $[2BF_3 \cdot MnO_4]^-$.

The kinetics were studied over a 30 °C temperature range. From the plot of ln K versus $1/T$, $\Delta H°$ and $\Delta S°$ for the equilibrium adduct formation (eq 1) are found to be 2.3 ± 0.5 kcal mol^{-1} and 21 ± 2 cal K^{-1} mol^{-1} respectively. The activation parameters $\Delta H^‡$ and $\Delta S^‡$ for the k step, obtained from the plot of ln k/T versus $1/T$, are 10.7 ± 1.3 kcal mol^{-1} and −22 ± 2 cal K^{-1} mol^{-1}, respectively.

The kinetics for the oxidation of c-C_6D_{12} were also investigated; $k_{C_6H_{12}}/k_{C_6D_{12}}$ was found to be 5.3 ± 0.6 at 25.0 °C, in good agreement with the value 4.7 ± 0.5 obtained by a competition method (vide supra).

Oxidation of Other Alkanes and Arylalkanes. The oxidation of other alkanes (c-C_5H_{12}, c-C_7H_{14}, and c-C_8H_{16}) has also been investigated. In all cases the corresponding ketone is the major product (Table 1).

The BF_3/$KMnO_4$ oxidation of various arylalkanes, including toluene, substituted toluenes, ethylbenzene, cumene, diphenylmethane, and triphenylmethane, has also been studied. No new absorption in the UV−vis region arises when $BF_3 \cdot CH_3CN$ is mixed with these aromatic compounds (in the absence of MnO_4^-) in CH_3CN, suggesting that there is negligible interaction between BF_3 and these substrates.

Table 1. Product Yields for the Oxidation of Hydrocarbons by $KMnO_4/BF_3$[a]

substrate	product[b] (% yield)
cyclohexane	cyclohexanol (8), cyclohexanone (73)
cyclooctane	cyclooctanol (4), cyclooctanone (76)
cyclopentane	cyclopentanol (11), cyclopentanone (39)
toluene	benzaldehyde (20)
ethylbenzene	acetophenone (45)
iso-propylbenzene	2-phenyl-2-propanol (26)
diphenylmethane	benzophenone (46)
triphenylmethane	triphenylmethanol (20)

[a] $KMnO_4$, 4.3×10^{-3} M; BF_3, 8.6×10^{-2} M; substrate, 1.0 M. $T = 23$ °C. Time = 5 min. All reactions were carried out in CH_3CN under argon. O_2 was strictly excluded from the reaction by four freeze−pump−thaw cycles. [b] The yields were calculated based on the system acting as a three-electron oxidant.

The product from the oxidation of toluene consists of 20% benzaldehyde, no change in the yield was observed and no benzoic acid was detected even after adding acidic iodide to reduce MnO_2 to Mn^{2+}. The detection limit of benzoic acid by GC under our conditions is around 5%. No products arising from benzene ring oxidation could be detected. Also no products such as methyl substituted diphenylmethanes or methylbenzophenone, which arise from the benzyl cation, could be found (detection limit < 1%), suggesting that $[BF_3{\cdot}MnO_4]^-$ does not oxidize toluene via a hydride abstraction mechanism.[23] The "unassisted" oxidation of toluene by $^n Bu_4NMnO_4$ produces predominantly benzoic acid;[17] such a difference in product distribution is probably due to a much faster rate of oxidation by $[BF_3{\cdot}MnO_4]^-$ than MnO_4^-.

The oxidation of ethylbenzene, isopropylbenzene, diphenylmethane, and triphenylmethane gave acetophenone (45%), 2-phenyl-2-propanol (26%), benzophenone (46%), and triphenylmethanol (20%), respectively. No other products could be detected.

The yields for the oxidation of the alkanes and arylalkanes by BF_3/MnO_4^- range from 20 to 80%. Lower yields are obtained for the oxidation of the arylalkanes, despite their lower C−H bond energies. Presumably further oxidation of the alcohol and ketone products occurs for these substrates, leading to unidentified ring degradation species. A similar result is also found for the unassisted oxidation of arylalkanes by $^n Bu_4NMnO_4$.[17]

Kinetic studies for the oxidation of these substrates by $KMnO_4/BF_3$ have also been carried out. For the oxidation of toluene, the rate law is the same as that of cyclohexane; k and K are found to be (9.22 ± 0.25) M^{-1} s^{-1} and (753 ± 42) M^{-1} respectively at 25.0 °C. The value of K is the same as that for cyclohexane, as expected if it represents the equilibrium constant for adduct formation, which should be independent of substrate. Notably, k, which represents the rate constant for the oxidation of toluene by $[BF_3{\cdot}MnO_4]^-$, is over 7 orders of magnitude larger than that by $^n Bu_4NMnO_4$ (4.2×10^{-7} M^{-1} s^{-1} at 25.0 °C).[17] $\Delta S^{\ddagger}$ values for the two pathways are similar, the much faster rate for the BF_3-activated pathway arises from a much lower $\Delta H^{\ddagger}$ (Table 2). On the other hand, the KIE for the BF_3-activated pathway, $k_{C_7H_8}/k_{C_7D_8} = 6.8 \pm 0.5$ (at 25.0 °C), is comparable to the value 6 ± 1 (at 45 °C) for the unactivated pathway.[17]

Table 2. Rates and Activation Parameters for the Oxidation of Toluene by $[BF_3{\cdot}MnO_4]^-$ and $^n Bu_4N[MnO_4]$

	$[BF_3{\cdot}MnO_4]^-$[a]	MnO_4^-[b]
rate constant at 298 K/M^{-1} s^{-1}	9.2	4.2×10^{-7}
$\Delta H^{\ddagger}$/kcal mol^{-1}	12.0 ± 0.6	21.0 ± 1.0
$\Delta S^{\ddagger}$/cal mol^{-1} K^{-1}	$-(14 \pm 3)$	$-(16 \pm 3)$
E_a/kcal mol^{-1}	12.6 ± 0.4	24.6 ± 0.9

[a] Reaction in CH_3CN. [b] Reaction in neat toluene. Data from ref 17.

Table 3. Representative Rate Data for the Oxidation of Hydrocarbons by $BF_3{\cdot}MnO_4^-$ [a]

substrate	k ($BF_3/KMnO_4$)/M^{-1} s^{-1}	BDE/kcal mol^{-1}
c-C_5H_{10}	6.90×10^{-1}	96.4[b]
c-C_6H_{12}	1.21	95.4[b]
c-C_7H_{14}	4.55	94.0[b]
c-C_8H_{16}	6.38	92.6[b]
$PhCH_3$	9.22	88.5[c]
$PhCH_2CH_3$	2.60×10^1	84.7[c]
$PhCH(CH_3)_2$	1.32×10^1	84.4[d]
Ph_2CH_2	1.36×10^2	82[c]
Ph_3CH	1.88×10^2	81[c]
p-$H_3CO-PhCH_3$	2.55×10^1	
p-$H_3C-PhCH_3$	4.55×10^1	
p-$Cl-PhCH_3$	5.85	

[a] $T = 298$ K, in CH_3CN. [b] Reference 26. [c] References 17 and 27. [d] Reference 28.

The kinetics for the oxidation of the other substrates were carried out at $[MnO_4^-] = 5 \times 10^{-5}$ M, [substrate] = 1×10^{-3}−2×10^{-1} M, and $[BF_3] = 2.0 \times 10^{-3}$ M. The k values were calculated from k_2 by using eq 5 with $K = 752$ M^{-1}. Results are shown in Table 3. The KIE for the oxidation of ethylbenzene is $k_{C_8H_{10}}/k_{C_8D_{10}} = 7.1 \pm 0.5$ (at 25.0 °C).

In the oxidation of various *para*-substituted toluenes, electron-donating substituents are found to cause an increase in rates while electron-withdrawing substituents cause a decrease in rates. Although the correlations are poor, the rates are monotonic with σ_p or σ^+ values, with $\rho = -(1.38 \pm 0.22)$ and $\rho^+ = -(0.69 \pm 0.25)$ (Figure S3). This is in contrast to oxidation by $^n Bu_4NMnO_4$ alone, where both electron-donating and electron-withdrawing substituents are found to cause an increase in rates.

Mechanism. Our results suggest that BF_3 forms an adduct with $KMnO_4$ in CH_3CN, which is the active species responsible for the oxidation of the hydrocarbons. This adduct is too reactive to isolate or characterize; however a number of much less-oxidizing metal-oxo species have been known to form stable adducts with boranes such as $B(C_6F_5)_3$.[24,25] The X-ray crystal structures of these adducts indicate that the boron is bonded to an oxo ligand, i.e., $M{=}O{-}B(C_6F_5)_3$. In general the B−O distance is consistent with a single bond, while there is substantial lengthening of the M=O bond. It is reasonable to assume that BF_3 also forms an adduct with MnO_4^- via bonding to an oxo ligand. Electron-withdrawing by the Lewis acidic BF_3 would enhance the oxidizing power of Mn^{VII}.

The rate-determining step (rds) in the oxidation of these substrates most likely involves H-atom abstraction by the adduct

(23) (a) Lockwood, M. A.; Wang, K.; Mayer, J. M. *J. Am. Chem. Soc.* **1999**, *121*, 11894−11895. (b) Larsen, A. S.; Wang, K.; Lockwood, M. A.; Rice, G. L.; Won, T.-J.; Lovell, S.; Sadílek, M.; Tureček, F.; Mayer, J. M. *J. Am. Chem. Soc.* **2002**, *124*, 10112−10123.

(24) Wolff, F.; Choukroun, R.; Lorber, C.; Donnadieu, B. *Eur. J. Inorg. Chem.* **2003**, 628−632.

(25) (a) Galsworthy, J. R.; Green, M. L. H.; Müller, M.; Prout, K. *J. Chem. Soc., Dalton Trans.* **1997**, 1309−1313. (b) Galsworthy, J. R.; Green, J. C.; Green, M. L. H.; Müller, M. *J. Chem. Soc., Dalton Trans.* **1998**, 15−19. (c) Doerrer, L. H.; Galsworthy, J. R.; Green, M. L. H.; Leech, M. A. *J. Chem. Soc., Dalton Trans.* **1998**, 2483−2487.

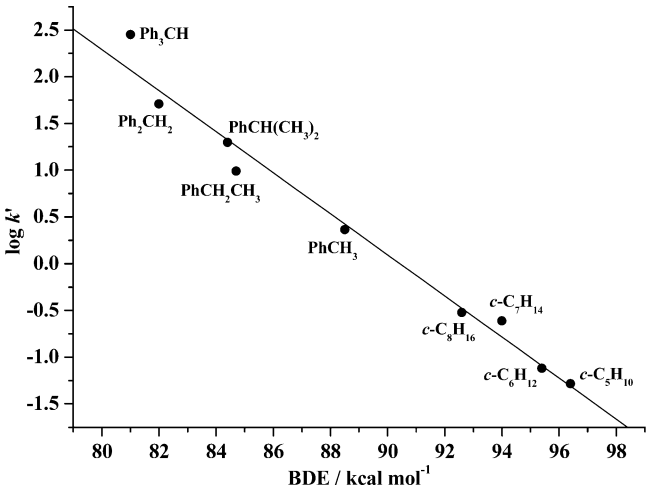

Figure 6. Plot of log k' vs BDE of the substrates for the BF_3 activated oxidation of hydrocarbons by MnO_4^- in CH_3CN at 298.0 K (slope = $-(1.94 \pm 0.11) \times 10^{-1}$, y-intercept = $(1.77 \pm 0.09) \times 10^1$, $r = -0.9900$).

to produce a carbon radical (eq 7), similar to oxidation by "unactivated" MnO_4^-.

$$[F_3B{-}OMn^{VII}(O)_3]^- + RH \rightarrow [F_3B{-}OMn^{VI}(O)_2(OH)]^- + R^\bullet \text{ slow} \quad (7)$$

$$[F_3B{-}OMn^{VI}(O)_2(OH)]^- + R^\bullet \rightarrow [F_3B{-}OMn^{V}(O)_2]^- + ROH \quad (8)$$

$OH^\bullet$ rebound to $R^\bullet$ will form ROH (eq 8), which is then rapidly oxidized to the corresponding aldehyde or ketone by $[F_3B{-}OMn^{V}(O)_2]^-$ and $[F_3B{-}OMn^{VII}(O)_3]^-$. The observation that O_2 affects the product yields is consistent with the formation of radicals in the rds.[29]

Correlation between Rate Constants and C−H Bond Strengths (BDE). Following the work of Mayer,[17] log k' is plotted against C−H BDE of the hydrocarbons. k' is k corrected for both the number of reactive hydrogen atoms in each substrate and the stoichiometry of the reaction.[30] A good linear correlation is found (Figure 6), which is consistent with a hydrogen atom transfer mechanism for the BF_3-activated oxidation of hydrocarbons by MnO_4^-. Similar correlations have been observed in the oxidation of hydrocarbons by CrO_2Cl_2,[31] ^{n}Bu$_4$NMnO$_4$,[17] and *trans*-$[Ru^{VI}(N_2O_2)(O)_2]^{2+}$ [32] and in the oxidation of phenols by *trans*-$[Ru^{VI}(N_2O_2)(O)_2]^{2+}$.[33] The rates of hydrogen atom transfer from arylalkanes to ^{n}Bu$_4$NMnO$_4$ also correlate with rates of abstraction by $OH^\bullet$, ^{t}BuO$^\bullet$, and ^{t}BuOO$^\bullet$.[17] If we assume that the rates of abstraction by BF_3/KMnO$_4$ also follow this correlation, then the O−H bond strength in $[F_3B{-}O{=}Mn^{VI}(O)_2(O{-}H)]^-$ can be estimated to be around 95 kcal/mol from the plot of log k vs the strength of the O−H bond formed by the oxidants.[17] This value is 15 kcal/mol larger than the O−H bond strength in HMnO$_4$ (80 kcal mol^{-1}).

Table 4. Reaction Barriers ($\Delta E^\ddagger$ in kcal/mol) and Reaction Energies (ΔE in kcal/mol) for the Three Reactions Calculated

	$\Delta E^\ddagger$	ΔE
reaction I	32.1	−34.2
reaction II	26.2	−38.2
reaction III	20.5	−56.9

Computational Study. The accelerating effect of BF_3 on the oxidation of alkanes by MnO_4^- has been studied computationally. A previous theoretical study[34] on the oxidation of CH_4 by MnO_4^- showed that the crucial step in the oxidation of CH_4 by MnO_4^- is the transformation of $MnO_4^- + CH_4 \rightarrow [O_2Mn(OH)(OCH_3)]^-$; the barrier for the transformation was calculated to be 32.3 kcal/mol. A hydrogen abstraction and oxygen rebound mechanism was postulated. The previous theoretical study also showed that the species involved in the reaction are well described by closed shell wave functions.[34] To examine the BF_3 accelerating effect, the following three model reactions were investigated with the aid of closed-shell self-consistent field (SCF) calculations.

Reaction I: $MnO_4^- + CH_4 \rightarrow [O_2Mn(OH)(OCH_3)]^-$

Reaction II: $MnO_4(BF_3)^- + CH_4 \rightarrow [O_2Mn(OH)(OCH_3)(BF_3)]^-$

Reaction III: $MnO_4(BF_3)_2^- + CH_4 \rightarrow [O_2Mn(OH)(OCH_3)(BF_3)_2]^-$

Geometry optimizations at the B3LYP level density functional theory,[35,36] with the 6-311+G** basis sets for the nonmetal atoms and the LanL2DZ basis sets for Mn,[37,38] have been performed to calculate the energies and structures of all species involved in the three reactions. The results of the calculations are listed in Table 4, the calculated transition states are shown in Figure 7, and the structural details of all the calculated species are given in the Supporting Information. The barrier for reaction I is calculated to be 32.1 kcal/mol, consistent with the result from the previous theoretical study,[34] while, in reactions II and III, the barriers are 26.2 and 20.5 kcal/mol, respectively. The lower barriers for reactions II and III explain the experimental observation that the oxidation of alkanes by MnO_4^- is accelerated by BF_3. The calculated barriers for methane oxidation are higher than the experimental values (Table 2) for toluene oxidation, as expected due to the higher C−H bond energy of methane (104.8 kcal/mol). It should also be noted the barriers for methane oxidation are gas-phase calculations, which should be somewhat different from the solution values.

(26) Luo, Y. R. *Handbook of Bond Dissociation Energies in Organic Compounds*; CRC Press: Boca Raton, FL, 2003.
(27) (a) Parker, V. D. *J. Am. Chem. Soc.* **1992**, *114*, 7458−7462. (b) Bordwell, F. G.; Cheng, J. P.; Ji, G. Z.; Satish, A. V.; Zhang, X. *J. Am. Chem. Soc.* **1991**, *113*, 9790−9795.
(28) *CRC Handbook of Chemistry and Physics*, 82nd ed.; Lide, D. R., Ed. CRC Press: Boca Raton, FL.
(29) The fact that the reaction rate is not affected may be due to more efficient trapping of $R^\bullet$ by O_2 than by Mn(VII) under our experimental conditions ([Mn(VII)] = 1×10^{-5}−5×10^{-5} M in kinetics studies).
(30) According to the proposed mechanism, the rate of disappearance of MnO_4^- in the reaction with cyclohexane should be 4/3 times the rate of hydrogen atom transfer, because $^4/_3$ mol of MnO_4^- are required to make 1 mol of cyclohexanone. Also there are 12 reactive H atoms in cyclohexane; hence $k' = k \times {}^1/_{12} \times {}^3/_4$. For Ph_3CH, however, the observed rate is only $^2/_3$ the rate of hydrogen atom transfer, since the product is Ph_3COH; in this case $k' = k \times {}^3/_2$. We thank one of the reviewers for pointing this out.
(31) Cook, G. K.; Mayer, J. M. *J. Am. Chem. Soc.* **1995**, *117*, 7139−7156.
(32) Lam, W. W. Y.; Yiu, S. M.; Yiu, D. T. Y.; Lau, T. C.; Yip, W. P.; Che, C. M. *Inorg. Chem.* **2003**, *42*, 8011−8018.
(33) Yiu, D. T. Y.; Lee, M. F. W.; Lam, W. W. Y.; Lau, T. C. *Inorg. Chem.* **2003**, *42*, 1225−1232.
(34) Strassner, T.; Houk, K. N. *J. Am. Chem. Soc.* **2000**, *122*, 7821−7822.
(35) (a) Becke, A. D. *J. Chem. Phys.* **1993**, *98*, 5648−5152. (b) Miehlich, B.; Savin, A.; Stoll, H.; Preuss, H. *Chem. Phys. Lett.* **1989**, *157*, 200−206. (c) Lee, C.; Yang, W.; Parr, G. *Phys. Rev. B* **1988**, *37*, 785−789.
(36) Frisch, M. J.; et al. *Gaussian 03*, revision B05; Gaussian, Inc.: Pittsburgh, PA, 2003.
(37) Hariharan, P. C.; Pople, J. A. *Theor. Chim. Acta* **1973**, *28*, 213−222.
(38) Hay, P. J.; Wadt, W. R. *J. Chem. Phys.* **1985**, *82*, 299−310.

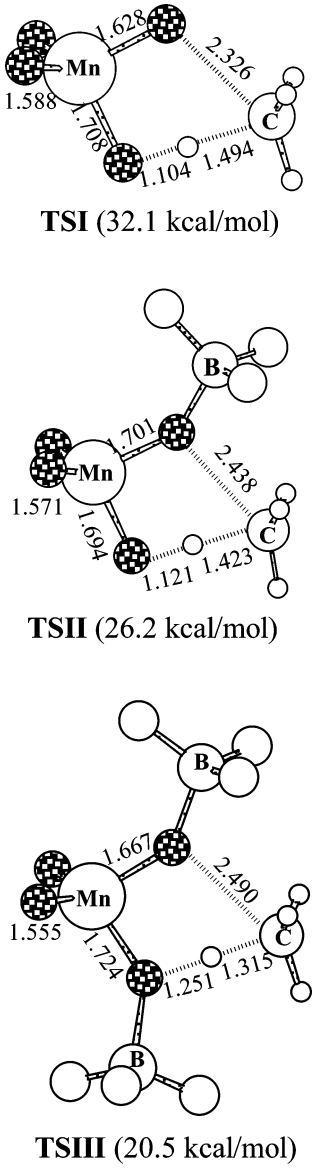

Figure 7. Optimized structures of transition states together with the reaction barriers. **TSI**, **TSII**, and **TSIII** are the transition states of reactions **I**, **II**, and **III**, respectively.

The calculated transition state structures (Figure 7) for the three reactions show no significant changes in the structural parameters related to the bond breaking and formation. The coordination of BF_3 makes the transition states earlier with respect to reactants. It should be noted that we also studied transition structures having other BF_3-coordination sites. In other words, transition structures in which BF_3 is coordinated to oxygens other than those shown in Figure 7 were calculated. The results of these calculations show that coordination to other sites has smaller effects in decreasing the reaction barrier. On the basis of the transition state structure for reaction I (**TSI**), we also calculated the single-point energy of its triplet state and found that the triplet state is less stable than the singlet state by 22.1 kcal/mol, further supporting that employing the closed-shell calculations is appropriate.

Figure 8 shows the plots[39] of the HOMO orbitals of the three transition states for the three reactions. Each HOMO orbital is

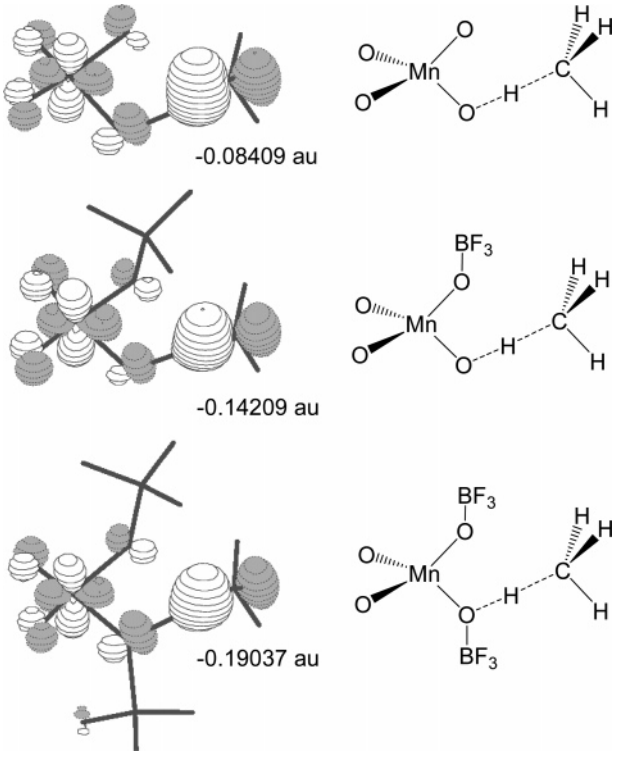

Figure 8. Spatial plots of the highest occupied molecular orbitals (HOMO), together with their orbital energies, for the three transition states of reactions **I**, **II**, and **III**.

extensively delocalized on both the metal center and the CH_3 group. In view of the significant contribution from the CH_3 group to each HOMO orbital in each transition state, we can envision that the H−CH_3 bond breaking is related to a hydrogen abstraction process, giving a radical CH_3 and a formal d^1 Mn(VI) center in the transition state. A similar hydrogen abstraction resulting in a radical pair species has been emphasized in a recent theoretical study of the methane activation on molybdenum oxides.[40]

The decrease in the reaction barriers resulted from the BF_3 coordination is driven by the increasing ability of the metal center to achieve a d^1 Mn(VI) electron configuration in the transition state. Figure 8 shows that significant Mn−O antibonding character can be found in each of the HOMOs. From the orbital energies shown in Figure 8, we can see that coordination of BF_3 significantly stabilizes the HOMOs and in turn facilitates the hydrogen abstraction process that passes the hydrogen's electron to the metal center. In other words, we can say that the BF_3 coordination to the lone pairs on the oxo groups reduces the antibonding character in the d orbital which accommodates the metal d electron in the transition state. Formally there are no d electrons in the metal center of MnO_4^-, and therefore the stabilizing effect to the reactant (MnO_4^-) is much less significant when compared with the transition state.

From the reaction energies shown in Table 4, we can see that binding the first BF_3 makes the reaction more favorable by 4.0 kcal/mol, slightly smaller than the stabilization energy (5.9 kcal/mol) gained by the transition state. However, binding the second BF_3 makes the reaction more favorable by 18.7 kcal/

(39) Schaftenaar, G. *Molden v3.5*; CAOS/CAMM Center Nijimegen: Toernooiveld, Nijimegen, Netherkands, 1999.

(40) (a) Fu, G.; Xu, X.; Lu, X.; Wan, H. *J. Am. Chem. Soc.* **2005**, *127*, 3989−3996. (b) Fu, G.; Xu, X.; Lu, X.; Wan, H. *J. Phys. Chem. B* **2005**, *109*, 6416−6421.

mol, significantly greater than the stabilization energy (5.7 kcal/mol) gained by the transition state. The steric repulsion between the Me and BF_3 groups in the product structure may significantly reduce the stabilization gained by binding the first BF_3. The steric effect is less important in the transition state structures.

Finally, we wish to point out that based on the calculation the lowest activation energy is achieved by the 2:1 adduct $[2BF_3{\cdot}MnO_4]^-$. Experimentally there is some evidence for this adduct; at $[BF_3] > 0.1$ M, the oxidation of cyclohexane becomes much faster than that expected for the 1:1 adduct $[BF_3{\cdot}MnO_4]^-$. Unfortunately the kinetics are irreproducible, thus preventing detailed studies.

Conclusion

BF_3 forms an adduct with MnO_4^- that oxidizes hydrocarbons at rates over 7 orders of magnitude faster than that by MnO_4^- alone. Experimental and computational studies support a hydrogen atom abstraction mechanism. The BF_3 accelerating effects have been attributed to a significant decrease in the reaction barriers resulting from the BF_3 coordination. The BF_3 coordination increases the ability of the Mn metal center to achieve a d^1 Mn^{VI} electron configuration in the transition state. The lowest activation energy is achieved by the 2:1 adduct $[2BF_3{\cdot}MnO_4]^-$.

Acknowledgment. The work described in this paper was supported by the Research Grants Council of Hong Kong (CityU 1097/01P) and the City University of Hong Kong (7001363). We thank the reviewers for valuable comments.

Supporting Information Available: Complete ref 35, table of rate data, UV/vis spectra, product yields, and the Cartesian coordinates of all the DFT calculated structures. This material is available free of charge via the Internet at http://pubs.acs.org.

JA0552951